4954–4962 Nucleic Acids Research, 1995, Vol. 23, No. 24

Efficient hammerhead ribozyme-mediated cleavage of the structured hepatitis B virus encapsidation signal *in vitro* and in cell extracts, but not in intact cells

Jürgen Beck and Michael Nassal*

Zentrum für Molekulare Biologie, Universität Heidelberg, Im Neuenheimer Feld 282, D-69120 Heidelberg, Germany

Received October 9, 1995; Revised and Accepted November 8, 1995

ABSTRACT

Hepatitis B virus (HBV), the causative agent of B-type hepatitis in man, is a small enveloped DNA virus that replicates through reverse transcription of an RNA intermediate, the terminally redundant RNA pregenome. An essential highly conserved *cis*-element present twice on this RNA is the encapsidation signal ε, a stem–loop structure that is critical for pregenome packaging and reverse transcription. ε is hence an attractive target for antiviral therapy. Its structure, however, is a potential obstacle to antivirals whose action depends on hybridization, e.g. ribozymes. Here we demonstrate effective *in vitro* cleavage inside ε by hammerhead ribozymes containing flanking sequences complementary to an adjacent less structured region. Upon co-transfection with a HBV expression construct corresponding ribozymes embedded in a U6 snRNA context led to a significant, though modest, reduction in the steady-state level of HBV pregenomes. Inactive ribozyme mutants revealed that antisense effects contributed substantially to this reduction, however, efficient ε cleavage by the intracellularly expressed ribozymes was observed in Mg^{2+}-supplemented cell lysates. Artificial HBV pregenomes carrying the ribozymes in *cis* and model RNAs lacking all HBV sequences except ε exhibited essentially the same behaviour. Hence, neither the absence of co-localization of ribozyme and target nor a viral component, but rather a cellular factor(s), is responsible for the strikingly different ribozyme activities inside cells and in cellular extracts.

INTRODUCTION

Hepatitis B virus (HBV) is a small hepatotropic DNA virus causing acute and chronic B-type hepatitis in man. Chronic infection is associated with a high risk of liver cirrhosis and, eventually, primary liver carcinoma. Currently available therapies are of limited efficacy (for a review see 1). HBV replication proceeds by an unusual protein priming mechanism (2–4), through reverse transcription of an RNA intermediate, the RNA pregenome (for a review see 5). While the pre-genome also serves as the mRNA for the capsid protein and the replication enzyme (P protein), its packaging into nucleocapsids and reverse transcription depend crucially on a *cis*-acting RNA element, the encapsidation signal ε (6). Comprising about 60 nt, ε is present close to the 5′-end of the pregenome and, due to a terminal redundancy, also at its 3′-end (see Fig. 4B). Its key roles in viral replication make ε an attractive target for antiviral therapy, e.g. by antisense or ribozyme approaches (for reviews see 7–9).

The functions of ε depend on a characteristic secondary structure (see Fig. 1A), a lower and upper stem with a bulge, a loop and a single unpaired U residue (10,11). The overall structure forms a binding site for P protein; two of the six bulge nucleotides appear to be directly involved in this interaction (12), while the 3′-proximal half of the bulge serves as the template for a short DNA oligonucleotide that, covalently bound to P protein, is used as a primer for first strand DNA synthesis (5). This structure might pose a problem to all approaches relying on hybridization between ε and a therapeutic nucleic acid, as target accessibility might be of importance (7). However, the high conservation of ε primary sequence (13,14), resulting from its multifunctionality and the requirement for secondary structure preservation, provides a distinct advantage regarding a serious problem in all antiviral therapies, the emergence of escape variants (for a review see 15). We therefore investigated the ability of various hammerhead ribozymes to specifically cleave ε after a GUC target triplet in the lower stem (see Figs 1A and 2). Cleavage *in vivo* should interfere with all HBV pregenome functions and, hence, with virus replication.

Hammerhead ribozymes (16) consist of a small catalytic core domain plus 5′- and 3′-flanking double helical regions (see Fig. 1B). Functional ribozyme structures (for a review see 17) also form *in trans* (18) and can be directed against foreign target sequences by providing the core domain with complementary flanking sequences (19). *In vitro* studies confirmed that increasing their length enhances the affinity for the target, but impedes multiple turnover. *In vivo*, however, the complex environment has so far precluded generalized predictions for optimal length (20). By varying the length of the flanking sequences we therefore first searched for ribozymes capable of efficiently cleaving the

* To whom correspondence should be addressed

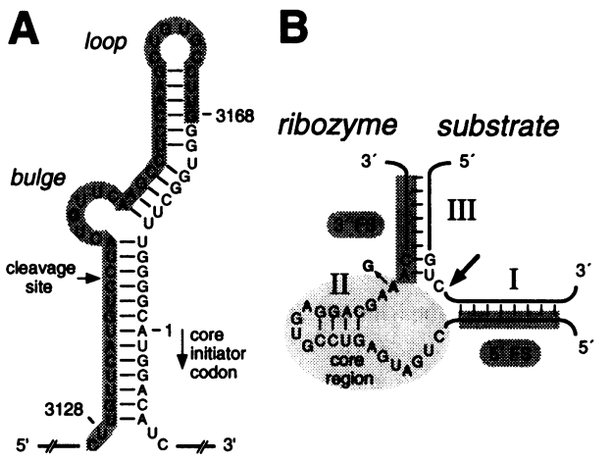

Figure 1. Structural characteristics of HBV target and ribozyme RNAs. (**A**) The HBV ε signal. The ε secondary structure, including the expected cleavage site after C3138, is shown. The ε sequence present in the model substrate $S_{\Delta\varepsilon}$ is shadowed. The core protein initiator codon is indicated by an arrow. (**B**) Generalized secondary structure model for hammerhead ribozymes. Hybridization of the ribozyme RNA containing the catalytic core region, derived from (+)sTRSV, and appropriate 5′- and 3′-flanking sequences (5′-FS and 3′-FS) with the substrate RNA generates a complex with double helical regions I–III. The arrow indicates the cleavage site. Replacement of A14 by G produces catalytically inactive ribozyme variants.

structured ε target *in vitro*. Next we transplanted these sequences into constructs allowing for high level expression in animal cells. As no feasible cell culture infection system is available for HBV, we assessed their effects by co-transfection of ribozyme and HBV expression constructs in human liver cell lines.

MATERIALS AND METHODS

Ribozyme constructs

All ribozyme-encoding plasmids contain the core domain from (+)-RNA of the satellite of tobacco ringspot virus (19) plus flanking regions complementary to the HBV sequence preceding and following the C residue in the GUC triplet at positions 3136–3138 (numbering system according to 21). Individual constructs were designated according to the length of their HBV-specific 3′- and 5′-flanks, e.g. rz10/9 is complementary to the 10 nt 5′ and 9 nt 3′ of C3138 (cf. Fig. 2). *Sac*I–*Eco*RI restriction fragments with the corresponding sequences were prepared from synthetic oligonucleotides or by PCR on appropriate templates. For *in vitro* transcription they were cloned into pBSIISK(–) (Stratagene, Heidelberg, Germany), yielding the pBSRz plasmids, and for transfection experiments into pU6Rz, each cut with the same enzymes. In the inactive ribozyme variants A14 (nomenclature according to 22) is replaced by a G residue. pU6Rz contains, in a pSP64-derived vector background, the human U6 snRNA promoter (23) as a 0.5 kb *Pst*I–*Eco*RV fragment (prepared by PCR on plasmid phU6.U1 provided by I.Mattaj), followed by a synthetic *Eco*RV–*Hin*dIII fragment encoding U6 snRNA-derived hairpin structures and *Sac*I–*Eco*RI sites for cloning of rz-encoding fragments (see Fig. 4A).

Target RNA constructs

Plasmid pCHG-3068-T7, used to generate HBV target RNAs *in vitro*, differs from the previously described plasmid pCHG-3122 (10) by a T7 promoter cassette inserted into the *Hin*dIII site and by containing HBV sequence from position nt 3068, rather than 3122. *In vitro* transcripts start with an additional 14 nt derived from the vector. In transfections the target RNA was provided by pCHT-9/3091 (24), in which transcription of an authentic 3.5 kb pregenome is driven by the CMV IE promoter and terminated by the HBV polyadenylation signal. For expression of HBV pregenomes carrying rz38/31 *in cis* plasmid pCRzHs (see Fig. 6A) was constructed by inserting the ribozyme-encoding sequence as a *Sma*I–*Eco*RV fragment into the filled-in *Sal*I site between the CMV promoter and the HBV sequence in pCHT-9/3091. In the control construct pCRzHas the orientation of the ribozyme sequence is reversed. Plasmid pCεluc (see Fig. 7A) served to express ε–luciferase fusion RNAs. The CMV IE promoter is followed by HBV sequence (nt 3091–11) linked to the luciferase open reading frame as present in plasmid pUHC131-1 (25). Transcripts start nominally at HBV position nt 3100 and terminate after a SV40 polyadenylation signal. In the translation product the first three amino acids of the HBV core protein replace the N-terminal two amino acids of luciferase. All relevant sequences

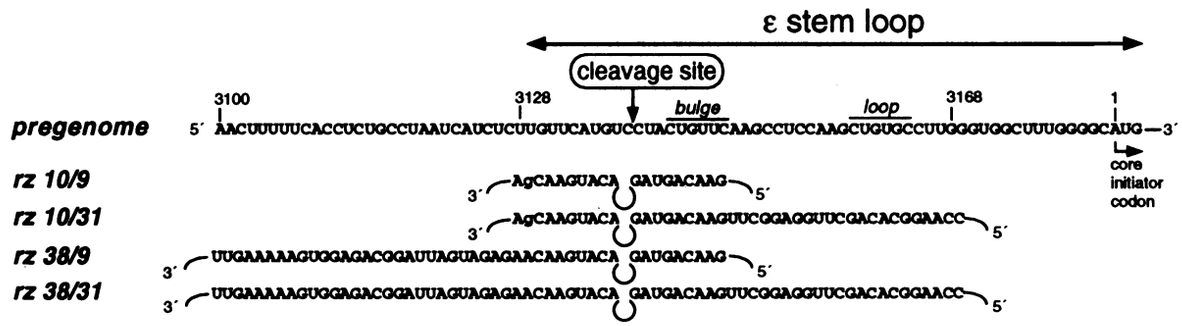

Figure 2. Alignment of ribozyme flanking sequences and the HBV target region. The 5′-terminal sequence of an authentic HBV pregenome (transcription start at nt 3100), including the location of secondary structure features, is shown in the first line, ribozymes with their designations being depicted below. The lower case g in rz10/9 and rz10/31 refers to a G-U pair. The central loop symbolizes the core region. Non-complementary vector-derived sequences on the *in vitro* transcripts (20 nt at the 5′-end and 3–5 nt at the 3′-end) are indicated by the curved lines; HBV-specific sequences in the *in vivo*-expressed ribozymes are identical, but contain different terminal sequences (see legend to Fig. 4).

where confirmed by sequencing with Sequenase (Amersham/USB, Braunschweig, Germany).

In vitro and *in vivo* expression of ribozyme and target RNAs

In vitro transcripts were prepared according to the supplier (Promega). Ribozymes were transcribed with T3 RNA polymerase (Stratagene) from pBSRz plasmids linearized with *Eco*RI, precipitated and redissolved in 50 mM Tris–HCl, pH 7.5, 1 mM EDTA at a final concentration of 10 pmol/µl. Radiolabelled substrates $S_{\Delta\varepsilon}$ and S_{ε} were transcribed with T7 RNA polymerase (Stratagene) from pCHG-3068-T7 linearized with *Sty*I or *Bgl*II respectively in the presence of [α-^{32}P]CTP (800Ci/mmol; Amersham). After gel purification the RNAs were dissolved in 50 mM Tris–HCl, pH 7.5, 1 mM EDTA at a final concentration of 1 pmol/µl. The specific activity was ~8×10^5 c.p.m./pmol. For *in vivo* expression target- and ribozyme-encoding plasmids were transfected into the human hepatoma cell line HuH7 using the calcium phosphate co-precipitation method as previously described (24). Usually 15 µg ribozyme construct, 3 µg target construct and, if desired, 5 µg CAT or β-Gal control plasmid were used per 10 cm culture dish.

Detection of ribozyme-mediated cleavage

In vitro assays were performed using 1 pmol substrate pre-equilibrated for 5 min at 37°C in reaction buffer (50 mM Tris–HCl, pH 7.5, 10 mM $MgCl_2$) and addition of 10 pmol ribozyme; the total volume was 10 µl. Aliquots of 1 µl were removed at various time points and added to 9 µl stop solution (95% formamide, 20 mM EDTA) on ice. Samples were analysed on denaturing polyacrylamide gels containing 6% polyacrylamide and 7 M urea. Band intensities were quantified using a PhosphorImager (Molecular Dynamics, Krefeld, Germany).

For analyses of RNAs from transfections cells were lysed 2 days post-transfection in 1 ml lysis buffer (10 mM HEPES, pH 7.5, 100 mM NaCl, 1 mM EDTA, 1% Nonidet P-40, 1 mM dithiothreitol, 10 U/ml RNasin) for 10 min at 4°C. After pelleting the nuclei 400 µl supernatant were treated with proteinase K (250 µg/ml) in the presence of 1% SDS for 30 min at 37°C. After phenol extraction and ethanol precipitation the pellet was washed in 70% ethanol and either directly dissolved in 20 µl hybridization buffer (80% formamide, 40 mM PIPES, pH 6.4, 400 mM NaCl, 1 mM EDTA) for RNase protection analysis or, for DNase digestion, incubated in 100 µl DNase buffer (10 mM HEPES, pH 7.5, 50 mM NaCl, 5 mM $MgCl_2$, 1 mM dithiothreitol, 40 U/ml RNasin) supplemented with 0.5 U RNase-free DNase (Boehringer, Mannheim, Germany) for 30 min at 37°C. After phenol extraction and isopropanol precipitation the pellet was washed with 70% ethanol and redissolved in 20 µl hybridization buffer. Radiolabelled antisense probes were generated *in vitro* as described above. About 50 000 c.p.m. gel-purified RNA were used per assay. The previously described 424 nt probe H (26) is complementary to the HBV sequence from positions nt 3007 to 245 (Fig. 4C). Probe H2 (417nt) is complementary to HBV from positions nt 429–760 and was obtained by T7 RNA polymerase transcription from a *Bam*HI-linearized plasmid containing a *Bsp*EI–*Bst*EII HBV fragment (after Klenow fill in) inserted in the *Eco*RV site of pBSIISK(–). Probe C, ~450 nt in length, is complementary to the 5′ proximal region of the *CAT* gene and yields a protected fragment of ~250 nt. Probe L consists of 572 nt, of which 475 nt are specific for a *Kpn*I–*Cfr*10I fragment from pCεluc (see Fig. 7A). The *lacZ*-specific probe Z, 559 nt long, is identical to the previously described probe 2 (10). Owing to a 2 nt insert in a *Cla*I site of the *lacZ* gene this probe yields two (226 and 206 nt) rather than one protected fragment when hybridized to wild-type *lacZ* RNA from pCMVβGal. Hybridizations and detection of the protected fragments on denaturing 6% polyacrylamide gels were performed as previously described (10).

Quantitation of ribozyme effects on target RNAs in transfected cells

Relative amounts of HBV-specific transcripts were measured by RNase protection using probes H and/or H2 and normalized to the signals obtained for the co-expressed *CAT* RNA with probe C. Luciferase-specific signals from the ε–luciferase model substrate, detected with probe L, were normalized to the *lacZ* signals obtained with probe Z from the co-transfected pCMVβGal plasmid. At the protein level ribozyme effects were measured by determining the relative luciferase versus β-galactosidase activities according to standard procedures (27).

RESULTS

In vitro screening for ribozymes capable of efficient ε-cleavage

Hammerhead ribozymes cleave their targets after triplets conforming to the consensus NUX (N = A, G, C or U, X = A, C or U; 28). Of several candidates we chose the GUC (nt positions 3136–3138) in the lower stem of ε as target (Fig. 1A). Corresponding ribozymes were obtained by *in vitro* transcription from pBSRz constructs carrying the core domain from (+)-strand RNA of the satellite of tobacco ringspot virus (sTRSV; Fig. 1B) flanked by sequences complementary to the HBV sequence surrounding the target triplet. Their lengths varied from 10 to 38 nt in the 3′-part of the ribozyme and from 9 to 31 nt in its 5′-part (Fig. 2). Target RNAs were produced *in vitro* from plasmid pCHG3068-T7, which contains HBV sequence from nt 3068 to 36, i.e. including the complete ε-signal, under control of the T7 promoter.

To assess the importance of target structure we compared, under single turnover conditions (ribozyme in 10-fold excess over target), cleavage of a 170 nt substrate containing the entire ε signal (S_{ε}) with that of a 3′-truncated RNA ($S_{\Delta\varepsilon}$) unable to form the stable ε structure. Ribozyme and target were incubated at 37°C in the presence of 10 mM Mg^{2+}. As detected by PAGE, all ribozymes cleaved both targets at the predicted site, as shown for rz38/9 and rz10/31 in Figure 3A; no cleavage products were detectable with the inactive point mutant rz38/9m (core nt A14→G). Cleavage efficiencies for all ribozymes were determined, using a PhosphorImager, from the ratio of cleaved versus the sum of cleaved plus uncleaved RNA and are summarized in Figure 3B. For the truncated target the lengths of the flanking sequences had no marked influence: after 20 min three of the four ribozymes had cleaved >90% of the $S_{\Delta\varepsilon}$ RNA; for rz10/31 this value was ~60%. Correspondingly, the times required to achieve 50% cleavage ($t_{1/2}$) varied from <5 min (rz10/9, rz38/31 and rz38/9) to ~10 min (rz10/31). For the full-length target S_{ε}, however, dramatic differences were observed: $t_{1/2}$ for cleavage by both ribozymes with a short 3′-arm (rz10/9 and rz10/31)

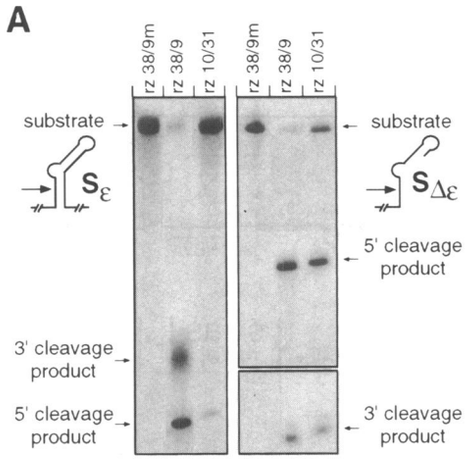

B

	cleaved fraction (%)		substrate half-life	
	S_ε	$S_{\Delta\varepsilon}$	S_ε	$S_{\Delta\varepsilon}$
rz 10/9	< 5	> 90	> 8 h[a]	~ 3 '
rz 10/31	~ 10	~ 60	> 2 h[b]	~ 10 '
rz 38/9	> 90	> 90	~ 3 '	~ 2 '
rz 38/31	~ 70	> 90	~ 8 '	~ 2 '

Figure 3. Dependence of cleavage efficiency *in vitro* on target structure and ribozyme flanking sequences. (**A**) Ribozyme-mediated cleavage of substrates S_ε and $S_{\Delta\varepsilon}$. Radiolabelled substrate RNAs (left, S_ε, right, $S_{\Delta\varepsilon}$, with symbolic representations of their secondary structures) were incubated with a 10-fold molar excess of the indicated *in vitro*-transcribed ribozyme RNA (see Materials and Methods for details). Products obtained after 20 min incubation were separated by denaturing PAGE and visualized using a PhosphorImager. The non-homogeneous appearance of the 3'-products is due to a 3'-terminal heterogeneity of the initial *in vitro* transcripts, resulting from non-templated nucleotide addition. (**B**) Summary of cleavage kinetics. Quantitated signal intensities on autoradiograms like those in (A) were used to calculate, for the indicated substrate/ribozyme combinations, the extent of cleavage after 20 min (ratio of cleaved versus cleaved plus uncleaved × 100); approximate substrate half-lives were determined from samples taken after various time points. [a]About 20% cleavage after 8 h; [b]~20% cleavage after 2 h.

increased to several hours. In contrast, the reaction rate for ribozyme rz38/9 was almost unchanged and that for rz38/31 only slightly increased to ~8 min. Hence target structure is important, in particular for reactions involving ribozymes with short flanks. However, efficient cleavage is feasible with appropriately lengthened flanking sequences. The strong effect of extending the 3'- but not the 5'-flank (e.g. rz38/9 versus rz10/31) correlates with its complementarity to the less structured HBV sequence 5' of ε.

Construction of a U6 snRNA promoter-based ribozyme expression vector

To investigate the anti-HBV activity of the above described ribozymes in living cells we sought an expression vector that would allow for high level transcription of short RNAs and in which any extra transcript sequences would not occlude the ribozyme part by intramolecular base pairing. We hence constructed the plasmids of the pU6Rz series (Fig. 4A): transcription is driven by the human U6 snRNA promoter, which, unlike many RNA polymerase III promoters, requires no signals in the transcribed region (23). The sequences flanking the ribozyme region are self-complementary; 5'-terminally they comprise, with

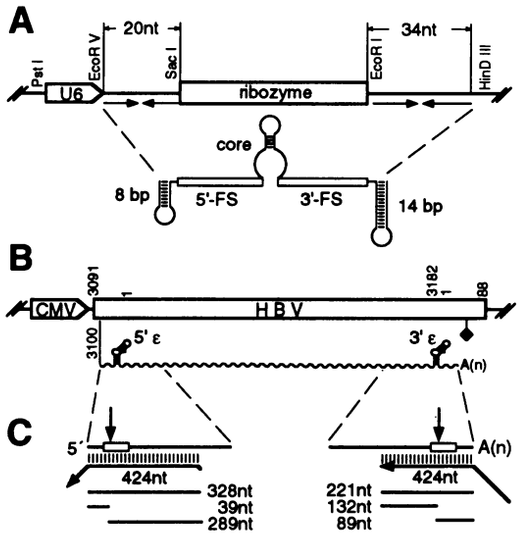

Figure 4. Ribozyme and target constructs analysed by transfection. (**A**) Schematic representation of pU6Rz-derived ribozyme transcripts. Plasmids of the pU6Rz series contain the human U6 snRNA promoter and a DNA cassette with unique restriction sites encoding the ribozyme core region (central stem–loop), HBV-specific flanks and terminal inverted repeats derived from U6 snRNA expected to fold into hairpins of 8 and 14 bp respectively. (**B**) Schematic representation of the HBV target construct. CMV promoter-driven transcription of the cloned overlength HBV genome produces an authentic, terminally redundant RNA pregenome with two ε copies. (**C**) Principle of RNase protection assay. The ε stem–loop is symbolized by a box, the antisense probe (probe H) by leftward pointing arrows. The expected sizes for protected probe fragments after hybridization to intact or ribozyme-cleaved 5' and 3' ε are indicated.

slight modifications, the proposed 5'-proximal stem–loop of U6 snRNA (29), including the authentic stable tetraloop consensus motif (UUCG; 30); the signals required for U6 snRNA nuclear import in *Xenopus laevis* oocytes (31) are absent. The 3'-part is derived from the basal half of the 3'-proximal U6 snRNA stem–loop; the distal half is replaced by another stable tetraloop (UACG). According to computer predictions these terminal hairpins fold independently of the presence of the ribozyme part. Transient expression in the human hepatoma cell line HuH7 yielded, until day 3 post-transfection, steady-state levels of 10^5–10^6 cytoplasmic copies of ribozyme per transfected cell, as estimated by RNAse protection assay from the intensities of ribozyme-specific signals in cell extracts compared with those of known amounts of *in vitro*-transcribed ribozymes and assuming transfection efficiencies of 1 or 10% respectively (data not shown).

Effects of anti-ε ribozymes in co-transfected hepatoma cell lines: moderate intracellular activity, but efficient post-lysis cleavage

To assess the potential of the ribozymes to intracellularly cleave HBV pregenomic RNA we co-transfected, into HuH7 cells, the pU6Rz plasmids with the HBV expression plasmid pCHT-9/3091 (24), which produces an overlength HBV RNA essentially identical to the authentic pregenome (Fig. 4B). As internal standard a third construct expressing the *CAT* gene was included; lacking any HBV sequence it should not be influenced by anti-ε

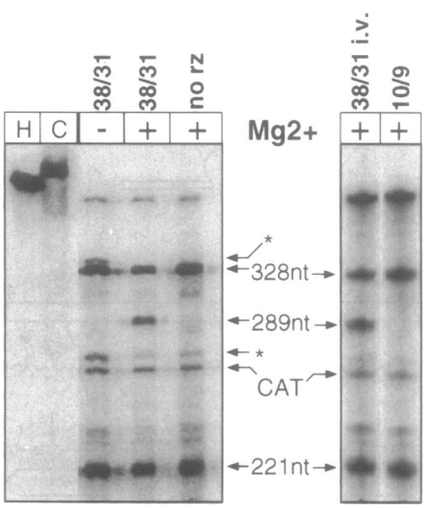

Figure 5. Post-lysis cleavage of the HBV pregenome by co-expressed ribozymes. Cytoplasmic RNA from cells transfected with or without the indicated ribozyme constructs was either prepared in the absence of Mg^{2+} or including a 30 min DNase treatment in the presence of 5 mM Mg^{2+}. HBV pregenome and *CAT* control RNA were simultaneously detected by RNase protection assay with probes H and C. Bands of 328 and 221 nt correspond to intact 5′ and 3′ ε. An additional band (nominally 289 nt) was exclusively produced in the presence of Mg^{2+} and rz38/31, but not rz10/9. Incubation of *in vivo*-expressed HBV RNA with *in vitro*-transcribed rz38/31 (lane 38/31i.v.) generated a signal of identical mobility. Signals marked with an asterisk occured only without DNase treatment and hence probably originate from plasmid DNA.

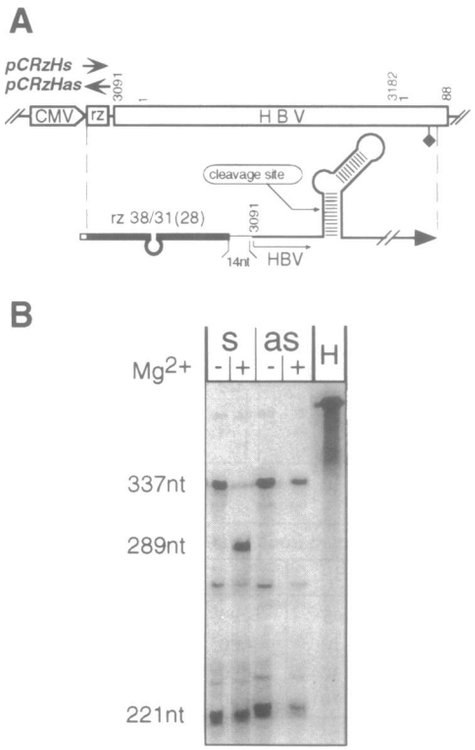

Figure 6. Post-lysis cleavage of the HBV pregenome by a *cis*-acting ribozyme. (**A**) Schematic structure of the artificial pregenome carrying rz38/31 *in cis*. A DNA cassette encoding rz38/31 (box marked rz) was inserted upstream of the cloned HBV genome either in the sense (pCRzHs) or antisense (pCRzHas) orientation. The 5′-terminal structure of the transcript is schematically shown below; the 5′-flank is expected to be reduced from 31 to 28 nt. (**B**) Analysis of intracellular and post-lysis cleavage by RNase protection. As in Figure 5, cytoplasmic RNA from cells transfected with either construct was analysed with or without DNase/Mg^{2+} treatment. Due to additional HBV nucleotides present in the transcripts (see A) the band corresponding to uncleaved 5′ ε is sligthly larger (337 nt) than with an authentic pregenome. The cleavage-specific signal (289 nt) appears only in the Mg^{2+}-treated sample with rz38/31 in the sense orientation (lane s+).

ribozymes. Control transfections were carried out with the parental pU6Rz plasmid lacking a ribozyme insert. Total cytoplasmic RNA, isolated by Nonidet P-40-mediated lysis, was analysed by RNase protection assays using antisense probes against two different regions of the pregenome (probes H and H2) and the *CAT* mRNA (probe C). Signal intensities were quantified using a PhosphorImager system.

A possible *in vivo* effect of the ribozymes might have been directly detectable by the appearance of specific cleavage products and/or by a reduction of HBV RNA in the ribozyme-producing cells. Probe H, covering the cleavage site (Fig. 4C), generated the two signals expected from hybridization to the uncleaved 5′ and 3′ ε sequences (bands of 328 and 221 nt respectively) in all samples. RNA from cells transfected with rz38/9 or rz38/31, however, yielded a further protected fragment (Fig. 5) that corresponded in size (nominally 289 nt) to the 3′ cleavage product of 5′ ε (the shorter band from a cleaved 3′ ε is not seen on this gel). The extra signal was absent from samples containing rz10/9, as well as rz10/31 and the inactive mutant rz38/9m (not shown). Furthermore, a fragment of identical mobility could be generated by adding *in vitro*-transcribed rz38/31 to the lysates of HBV-transfected cells (Fig. 5, lane 38/31i.v.). Hence all evidence supports the signal having arisen from a specific cleavage product. Its intensity, however, was rather surprising. The original protocol used for cytoplasmic RNA preparation consisted of proteinase K digestion and phenol extraction of clarified detergent lysates and included DNase digestion in the presence of 5 mM Mg^{2+}. Suspecting that cleavage could have occurred post-lysis, we analysed RNA prepared from the co-transfected cells in the complete absence of Mg^{2+}. As shown in Figure 5 (lane $-Mg^{2+}$), no specific cleavage products could be detected. Hence ribozyme-mediated cleavage had happened during incubation of the cell lysates in the presence of Mg^{2+}, but prior to hybridization with the probe. Quantitation of the band intensities showed post-lysis cleavage to be rather efficient: within 30 min at 37°C in buffer containing 5 mM Mg^{2+} ~35% of the endogenous target RNA was cleaved by the co-expressed ribozyme rz38/31 (Fig. 5 and Table 1); this value increased to ~50% cleavage after 1 h. Cleavage was not restricted to completely deproteinized RNA preparations, but occurred also upon adding 10 mM Mg^{2+} directly to the detergent extracts, though with lower efficiency (~10% rz38/31-mediated cleavage after 30 min; see also below).

We next sought to demonstrate *in vivo* activity of the ribozymes by measuring the steady-state levels of HBV RNA in the presence and absence of ribozyme. To account for differences in transfection efficiency the RNase protection assay signals for HBV were normalized to the signal from the co-transfected *CAT* construct (data summarized in Table 1). In four independent experiments using the ε-spanning probe H we observed a reduction to 75 ± 1% of the pregenome level without ribozyme in the presence of rz38/31. This result was confirmed with probe H2, which does not

overlap with ε. Essentially the same reduction was seen for rz38/9 (to 75 ± 4%), but not for rz10/9 and rz10/31, which were only poorly active *in vitro*. Notably, the inactive point mutant rz38/31m also led to a reduction (to 84 ± 4%).

Table 1. Effects of anti-ε ribozymes on the HBV target *in vivo* and post-lysis

Construct	Probe	HBV RNA level[a] (%)	*n*	Post-lysis[b] cleavage (%)
rz10/9	H	113 ± 8	4	0
rz10/31	H	109 ± 4	2	0
rz38/9	H	75 ± 4	2	~25
rz38/31	H	75 ± 1	4	~35
rz38/31	H2	76 ± 1	2	n.a.
rz38/31m	H	84 ± 4	4	0

[a]Relative HBV target levels in cells co-transfected with the indicated ribozyme construct were measured by quantitative RNase protection assay and are normalized to the signal in cells transfected with pU6Rz containing no ribozyme insert. Values are given as mean ± SD from *n* independent determinations.
[b]Extent of cleavage after 20 min DNase treatment in Mg^{2+}-containing buffer; n.a., not applicable.

These data demonstrate that co-expression of the HBV target RNA with ribozymes able to effectively cleave ε *in vitro* induces a moderate, but reproducible, reduction in the steady-state level of HBV pregenome. Reduction is, at least in part, due to antisense effects (rz38/31m), but cleavage may contribute to its extent. However, we have no direct evidence for cleavage *in vivo*. Conversely, HBV RNA was rather efficiently cleaved by the ribozymes after isolation from co-transfected cells. Hence the amount of intracellularly produced ribozyme is sufficient to cleave a substantial fraction of the co-expressed target RNA and ε can be cleaved not only on short model RNAs, but also in the context of the complete HBV pregenome. The apparent discrepancy between *in vivo* and post-lysis cleavage suggested some kind of inhibition of intracellular ribozyme activity. Candidate factors included a different subcellular localization of ribozyme and pregenome, occlusion of sequences required for hybridization of both RNAs by viral or cellular factors and suboptimal ionic conditions. Several of these possibilities were tested in the experiments described below.

Efficient post-lysis, but not intracellular, self-cleavage of a HBV pregenome carrying rz38/31 in *cis*

Problems owing to different subcellular localizations of ribozyme and target should be overcome if both were present on the same molecule. Plasmid pCRzHs38/31 (Fig. 6A) yields a chimeric RNA carrying rz38/31 in front of the complete HBV pregenome. Construct pCRzHas38/31, with the orientation of the ribozyme-encoding region reversed, served as control. After transfection and Mg^{2+}-free RNA preparation RNase protection assays with probe H gave no indication of intracellular cleavage with either construct (Fig. 6B). However, efficient post-lysis cleavage was observed when RNA in Nonidet P-40 extracts from cells transfected with construct pCRzHs38/31 was incubated under various conditions. The reaction was dependent on the presence of Mg^{2+} and on the correct orientation of the ribozyme part in the chimeric RNA. After 15 min at 37°C completely deproteinized RNA (proteinase K-digested plus phenol-extracted) was cleaved to ~90% in the presence of 10 mM Mg^{2+} (Fig. 6B) and to ~50% at 1 mM Mg^{2+}. However, deproteinization was not essential, as directly supplementing the lysate with 10 mM Mg^{2+} led to ~70% cleavage after 15 min incubation. Thus the chimeric RNA, once removed from the intracellular enviroment, has a high propensity to self cleave, even at almost physiologically low Mg^{2+} concentrations (47). A different subcellular localization of ribozyme and target is apparently not the major factor reponsible for *in vivo* inhibition of anti-ε ribozyme activity.

Post-lysis, but not intracellular, cleavage in the absence of HBV gene products

The multiple functions of the HBV pregenome require its interaction with P and core protein, which may interfere with hybridization of the ribozymes. In plasmid pCεluc (32) all HBV sequences except 5′ ε are replaced by the luciferase gene (Fig. 7A). HuH7 cells were co-transfected with pCεluc and several of the ribozyme expression constructs; for quantitation of the steady-state levels of target RNA in the presence and absence of ribozymes signal intensities were normalized to co-expressed β-galactosidase RNA. The results paralleled those seen with the HBV pregenome (Fig. 7C). The levels of luciferase RNA were moderately reduced in the presence of rz38/31 (to ~70% of that without ribozyme) and rz38/9 (to ~60%). In contrast, rz10/9 had no detectable effect, while the inactive point mutant rz38/9m also induced a substantial reduction (to ~60%). No specific cleavage products could be detected after RNA preparation in the absence of Mg^{2+}, while cleavage was easily detectable when RNA from deproteinized lysates was incubated with Mg^{2+} (Fig. 7B). We also determined the relative luciferase activities in the lysates (Fig. 7C). In agreement with the RNA analyses, those ribozymes inducing a reduction in the level of luciferase RNA led to decreased luciferase activity; both values appeared to be proportional, though the reduction in enzyme activity was more pronounced.

The clear correspondence between the ribozyme effects on authentic HBV target and the luciferase model substrate indicates that viral proteins are not the crucial factor responsible for intracellular ribozyme inhibition. The lack of detectable *in vivo* cleavage products, the steady-state RNA level reduction also by inactive ribozymes and the larger influence on enzyme activity than on RNA suggest that most of the *in vivo* ribozyme effects are due to an antisense mechanism. However, the post-lysis cleavage data again demonstrate the high intrinsic cleavage potential of the anti-ε ribozymes.

DISCUSSION

The lack of a generally applicable therapy for chronic hepatitis B and the severity of the disease call for novel therapeutic approaches. Ribozymes offer a similar target specificity to antisense strategies (for a review see 33) and, furthermore, the principal advantages of irreversible target destruction and multiple turnover (7–9). After earlier *in vitro* investigations, including HBV-derived targets (34,35), recent studies have produced encouraging data pertaining to the *in vivo* applicability of ribozymes (36); generalizations, however, are still questionable (37). In particular, direct experimental evidence for cleavage-dependent, as opposed to antisense-mediated, *in vivo* effects

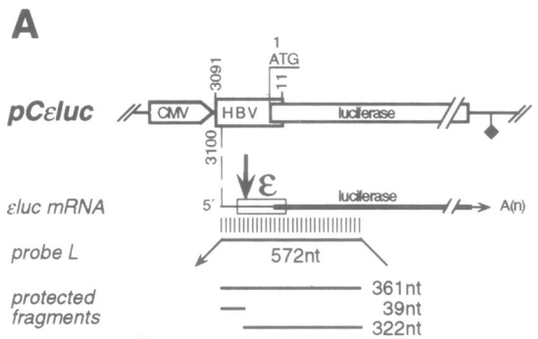

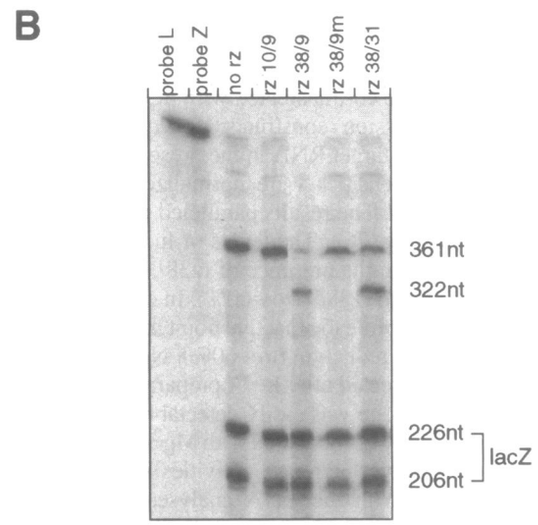

C

construct	rel. mRNA level (%)	n	rel. luciferase activity (%)	n
rz 10/9	101 ± 6	2	116 ± 19	9
rz 10/31	n.d.	-	94 ± 4	2
rz 38/9	58 ± 19	2	29 ± 5	9
rz 38/9m	59	1	31 ± 3	9
rz 38/31	72 ± 5	2	47 ± 11	11
rz 38/31m	n.d.	-	45 ± 2	5

Figure 7. Effect of ribozyme co-expression in the absence of HBV gene products. (**A**) Schematic structure of the ε–luciferase construct. In plasmid pCεluc the luciferase gene replaces the HBV genome downstream of ε; translation starts with the first three amino acids of HBV core protein and, hence, in an authentic context. Protected fragments from hybridization of probe L to the intact or cleaved ε–luciferase RNA are indicated below. (**B**) RNase protection analysis of ε–luciferase RNA after co-expression with various anti-ε ribozymes. ε–luciferase RNA in DNase-treated extracts from cells transfected with pCεluc and pU6Rz carrying no or the indicated ribozyme construct was detected with probe L. As an internal reference *lacZ* RNA from co-transfected pCMVβGal was simultaneously detected with probe Z. A specific cleavage product (322 nt) was only seen in samples expressing the active ribozyme variants rz38/9 and rz38/31. (**C**) Ribozyme effects on steady-state levels of ε–luciferase RNA and luciferase acitivity. mRNA levels were determined by normalization to the *lacZ* RNA signals and are given in relation to the sample containing no ribozyme. Luciferase activities were measured luminometrically and are normalized to the β-galactosidase activity in the same sample. *n*, number of individual determinations; n.d., not determined.

remains scarce. Amongst other problems, like specificity and efficiency of ribozyme delivery and expression (7–9), selection of the appropriate complementary regions on the target RNA, as well as predicting the optimal lengths of the ribozyme flanks, are as yet unresolved issues. Regions buried in intramolecular structures may be difficult to attack (38), however, extrapolations to the *in vivo* efficacy of a given ribozyme are problematic, owing to the difficulties in predicting large secondary structures in the complex intracellular environment. Another, probably severe, problem, in particular for targets derived from viruses with error-prone RNA-based replication strategies, is the selection of escape variants (15). For instance, a single point mutation in the centre of the hammerhead ribozyme consensus triplet NUX would render a virus cleavage resistant. With respect to therapeutic application, functionally important secondary structures displaying high sequence conservation are, therefore, attractive candidate targets. Our study of hammerhead ribozymes directed against the HBV ε signal revealed that structure-dependent cleavage inhibition could be overcome *in vitro* by appropriately extending the 3′-flanking sequences; in transfected cells ribozymes with high *in vitro* activity induced a significant reduction in the level of co-expressed HBV pregenome. However, reduction was at least in part due to antisense mechanisms and only moderate when compared with the extensive cleavage that occurred once ribozyme and target were removed from the intracellular environment, indicating that most of the ribozymes' intrinsic cleavage potential is masked inside the cell.

Hammerhead ribozyme-mediated cleavage of a structured target *in vitro*

Our *in vitro* data using ε targets with differing potential for secondary structure formation confirm the profound influence structure can have on the efficacy of ribozyme-mediated cleavage, likely by interfering with formation of a productive ribozyme–substrate complex. Under single turnover conditions the truncated target $S_{\Delta\varepsilon}$ was efficiently cleaved by all ribozymes tested. In contrast, striking differences were observed with the complete, structured target S_{ε}. Reaction times for 50% cleavage increased from minutes to several hours for the ribozymes with two short flanks (rz10/9). Lengthening the 3′-flank (rz38/9), but not the 5′-flank (rz10/31), enabled efficient cleavage. No further improvement was achieved by having two long flanks (rz38/31). The pyrimidine-rich 5′-terminal pregenome region preceding ε is probably little structured and may therefore provide an accessible region to initiate hybridization of those ribozymes having long 3′-flanks. In contrast, the entire region complementary to the ribozyme 5′-arms tested is involved in base pairing, except for the single-stranded bulge and loop. Apparently these are not sufficient to nucleate productive annealing. Hence, including in the targeted sequence an adjacent non-structured element may be a general means of achieving cleavage of structured targets.

Effect of anti-ε ribozymes in transfected cells

For producing short transcripts polymerase III promoters offer several advantages (9). The U6 snRNA promoter in our ribozyme constructs gave rise to 10^5–10^6 transcripts per transfected cell, in accord with a recent independent report (39). The additional U6 snRNA-derived sequences present in the ribozyme RNAs did not apparently interfere with productive annealing to the target, as demonstrated by their efficacy in post-lysis cleavage (see below).

In addition, *in vitro* transcripts corresponding to those produced by transfection exhibited a similar activity to the original *in vitro* constructs (not shown).

In co-transfections with the HBV target construct ribozymes capable of efficient ε cleavage *in vitro* led to a decrease of ~25% in the steady-state level of target RNA. Though an exact quantitation is difficult owing to the complex experimental scheme, we are confident from the reproducibility and specificity of the data that they reflect a true ribozyme-dependent reduction. Also, very similar results were obtained with an ε–luciferase model substrate (see below). Two major questions arise from these experiments: is the reduction dependent on ribozyme-mediated cleavage or an antisense effect and why is its extent only moderate?

The results with inactive ribozyme mutants point to a significant contribution of antisense effects, both with the HBV pregenome and the ε–luciferase model substrate. Possibly such hybrids are degraded by cellular nucleases. An additional translation inhibition is likely from the more pronounced effect on luciferase activity than on ε–luciferase RNA. These data, however, do not rule out some contribution to target RNA reduction by ribozyme-mediated cleavage and rapid degradation of the resulting fragments.

Most of the published evidence for *in vivo* cleavage activity of ribozymes is indirect. For instance, addition of a hammerhead domain enhanced inhibition of HIV-1 replication compared with the parental antisense RNA (40). Only a few reports describe the direct detection of intracellular cleavage products (37,41–43) and, with rare exceptions, PCR-based methods had to be employed to achieve sufficient sensitivity. Surprised by the high intensity of cleavage-specific signals in our initial RNase protection assays we examined each step after cell lysis and before gel electrophoresis for cleavage promoting conditions. As suspected, DNase treatment in the presence of Mg^{2+}, commonly used to remove the input plasmid prior to RNase protection in DNA transfection experiments, was the critical step. Omitting this step we found no evidence for *in vivo* cleavage by the anti-ε ribozymes. Thus most of the observed reduction in the steady-state level of HBV pregenomes may be due to antisense effects. The efficiency of post-lysis cleavage during incubation with Mg^{2+}, even for only minutes, emphasizes that inferences on the intracellular origin of cleavage products from such experiments have to be drawn with extreme caution, in particular when very sensitive detection methods are used, as was recently anticipated by others (42). It also indicates an intrinsically high cleavage potential of the *in vivo*-produced ribozymes, which is, however, largely masked inside the cell.

A second reason for the only modest effects we observed *in vivo* is inherent in the assay format. In transfection, which we had to use as a substitute for infection, the target is transcribed from a foreign promoter. Synthesis of new HBV RNA pregenomes is therefore independent of the normal HBV replication cycle and would not be terminated, even if an entire generation of pregenomes was eliminated by the ribozyme. Other studies reporting a significant inhibition of virus replication often used infection, at low multiplicity of infection, of target cells containing the ribozyme (44,45), therefore, the preformed ribozymes had to inactivate only one or a few incoming virus genomes.

Intracellular inhibition of anti-ε ribozyme activity

The post-lysis cleavage reaction in detergent extracts of co-transfected cells, specific for the active ribozyme variants, was most efficient after proteinase K treatment and phenol extraction. However, significant cleavage was also observed by directly supplementing the lysates with $MgCl_2$, as is particularly evident from the efficient self-cleavage of the *cis*-ribozyme construct. Attempting to define the nature of the intracellular block in ribozyme activity implied by the vastly different results in lysates versus intact cells we tested for possible influences of co-localization and viral gene products. The compartmentalization of eukaryotic cells has been recognized as a potential problem (9). Cotten *et al.* (46), analysing tRNA-embedded ribozymes in *X.laevis* oocytes, showed that low *in vivo* but high *in vitro* activity correlated with different subcellular localizations of both RNAs. However, pregenome transcripts carrying the ribozyme *in cis* gave generally the same result as co-transfections: *in vivo* cleavage products were not detectable, but efficient cleavage occured in cell extracts. Together these data suggest that *in vivo* inhibition is not predominantly caused by a different intracellular localization of ribozyme and target.

Proteins bound to ribozyme and/or target may shield regions required for productive interactions. P and, possibly, core protein interact with ε during HBV pregenome encapsidation. However, an ε-luciferase model target lacking all other HBV-specific sequences gave essentially the same results as the authentic pregenome. Though not ruling out the possibility that binding of viral factors to ε contributes to cleavage inhibition, these data imply crucial involvement *in vivo* of at least one other non-viral factor. This could be the absence of a general factor required for ribozyme activity and/or the presence of an inhibitory principle inside the cells, plausibly cellular proteins that bind to ε, the ribozyme or both.

One possible limiting general factor is Mg^{2+}. Efficient post-lysis cleavage was observed in lysates supplemented with 5 or 10 mM Mg^{2+}, the standard concentration in most *in vitro* experiments, while less cleavage occurred at the physiologically more relevant concentration of 1 mM Mg^{2+} (47). As, for therapeutic applications, it will be difficult to increase the intracellular Mg^{2+} level, selection experiments may provide access to ribozymes with lowered Mg^{2+}-requirements.

That post-lysis cleavage was most efficient after proteinase K treatment and phenol extraction suggests that cellular proteins may inhibit ribozyme–target hybridization, however, the non-ionic detergent Nonidet P-40 alone appeared sufficient to disrupt at least a part of such putative interactions. Proteins binding to hammerhead ribozymes have recently been described, however, the interaction was not specific for the core domain (48). Hence cellular proteins binding to the ε target may be more likely candidates. UV cross-linking experiments suggest that such proteins indeed exist (49; S.Perri and D.Ganem, personal communication). Once characterized, analysis of their potential role in inhibiting *in vivo* cleavage may be amenable to *in vitro* studies.

In summary, our data demonstrate that structured RNA regions, frequently of functional importance, should not *a priori* be ignored as antiviral targets, in particular with viruses having a high escape potential. Whether the vast difference in intracellular versus post-lysis ribozyme activity we have observed is a peculiarity of the specific target (e.g. cellular ε binding proteins) or pertains to a general problem for the ribozyme approach (e.g. insufficient intracellular Mg^{2+} activity) is currently not clear. However, the reduction in the steady-state levels of HBV pregenomes observed in our co-transfection assays encourages

further studies under the more natural, and probably more favourable, conditions of infection. Until an *in vitro* infection system for HBV becomes available the related duck hepatitis B virus (DHBV) may provide a feasible model system.

ACKNOWLEDGEMENTS

We thank Drs Iain Mattaj and Hermann Bujard for providing plasmids phU6.U1 and pUHC131 and Susanne G.Schaaf for plasmid pCεluc. This work was supported by grant Na 154/3-1 from the Deutsche Forschungsgemeinschaft.

REFERENCES

1 Lok,A.S.F. (1994) *J. Viral Hepatitis*, **1**, 105–124.
2 Wang,G.H. and Seeger,C. (1993) *J. Virol.*, **67**, 6507–6512.
3 Tavis,J.E. and Ganem,D. (1993) *Proc. Natl. Acad. Sci. USA*, **90**, 4107–4111.
4 Nassal,M. and Rieger,A. (1996) submitted for publication.
5 Nassal,M. and Schaller,H. (1993) *Trends Microbiol.*, **1**, 221–226.
6 Junker-Niepmann,M., Bartenschlager,R. and Schaller,H. (1990) *EMBO J.*, **9**, 3389–3396.
7 Sczakiel,G. and Nedbal,W. (1995) *Trends Microbiol.*, **3**, 213–217.
8 Kientopf,M., Esquivel,E.L., Brach,M.A. and Herrmann,F. (1995) *Lancet*, **345**, 1027–1031.
9 Rossi,J.J. (1995) *Trends Biotechnol.*, **13**, 301–306.
10 Knaus,T. and Nassal,M. (1993) *Nucleic Acids Res.*, **21**, 3967–3975.
11 Pollack,J.R. and Ganem,D. (1993) *J. Virol.*, **67**, 3254–3263.
12 Rieger,A. and Nassal,M. (1995) *Nucleic Acids Res.*, **23**, 3909–3915.
13 Laskus,T., Rakela,J. and Persing,D.H. (1994) *Virology*, **200**, 809–812.
14 Lok,A.S.F., Akarca,U. and Greene,S. (1994) *Proc. Natl. Acad. Sci. USA*, **91**, 4077–4081.
15 Coffin,J.M. (1995) *Science*, **267**, 483–489.
16 Symons,R.H. (1992) *Annu. Rev. Biochem.*, **61**, 641–671.
17 Dudna,J.A. (1995) *Structure*, **3**, 747–750.
18 Uhlenbeck,O.C. (1987) *Nature*, **328**, 296–600.
19 Haseloff,J. and Gerlach,W.L. (1988) *Nature*, **334**, 585–591.
20 Crisell,P., Thompson,S. and James,W. (1993) *Nucleic Acids Res.*, **21**, 5251–5255.
21 Pasek,M., Goto,T., Gilbert,W., Zink,B., Schaller,H., MacKay,P., Leadbetter,G. and Murray,K. (1979) *Nature*, **282**, 575–579.
22 Hertel,K.J., Pardi,A., Uhlenbeck,O.C., Koizumi,M., Ohtsuka,E., Uesugi,S., Cedergren,R., Eckstein,F., Gerlach,W.L., Hodgson,R. and Symons,R.H. (1992) *Nucleic Acids Res.*, **20**, 3252.
23 Hamm,J. and Mattaj,I.W. (1990) *Cell*, **63**, 109–118.
24 Nassal,M. (1992) *J. Virol.*, **66**, 4107–4116.
25 Bonin,A.L., Gossen,M. and Bujard,H. (1994) *Gene*, **141**, 75–77.
26 Nassal,M., Junker-Niepmann,M and Schaller,H. (1990) *Cell*, **63**, 1357–1363.
27 Ausubel,F.M. *et al.* (1995) *Current Protocols in Molecular Biology*. John Wiley & Sons, New York, NY.
28 Ruffner,D.E., Stormo,G.D. and Uhlenbeck,O.C. (1990) *Biochemistry*, **29**, 10695–10702.
29 Rinke,J., Appel,B., Digweed,M. and Lührmann,R. (1985) *J. Mol. Biol.*, **185**, 721–731.
30 Wyatt,J.R. and Tinoco,I.,Jr (1993) In Gesteland,R.F. and Atkins,J.F. (eds), *The RNA World*. Cold Spring Harbor Laboratory Press, Cold Spring Harbor, NY, pp. 465–496.
31 Hamm,J. and Mattaj,I.W. (1989) *EMBO J.*, **8**, 4179–4187.
32 Schaaf,S.G. (1995) Diploma thesis, University of Heidelberg, Heidelberg, Germany.
33 Whitton,J.L. (1994) *Adv. Virus Res.*, **44**, 267–303.
34 Offensperger,W.B., Blum,H.E. and Gerok,W. (1994) *Clin. Invest.*, **72**, 737–741.
35 von Weizsäcker,F., Blum,H.E. and Wands,J.R. (1992) *Biochem. Biophys. Res. Commun.*, **189**, 743–748.
36 Yu,M., Poeschla,E. and Wong-Staal,F. (1994) *Gene Therapy*, **1**, 13–26.
37 Bertrand,E., Pictet,R. and Grange,T. (1994) *Nucleic Acids Res.*, **22**, 293–300 (erratum **22**, 1326).
38 Xing,Z. and Whitton,J.L. (1992) *J. Virol.*, **66**, 1361–1369.
39 Noonberg,S.B., Scott,G.K., Garovoy,M.R., Benz,C.C. and Hunt,C.A. (1994) *Nucleic Acids Res.*, **22**, 2830–2836.
40 Homann,M., Tzortzakaki,S., Rittner,K., Sczakiel,G. and Tabler,M. (1993) *Nucleic Acids Res.*, **21**, 2809–2814.
41 Steinecke,P., Herget,T. and Schreier,P.H. (1992) *EMBO J.*, **11**, 1525–1530.
42 Ferbeyre,G., Bratty,J., Chen,H. and Cedergren,R. (1995) *Gene*, **155**, 45–50.
43 Cantor,G.H., McElwain,T.F., Birkebak,T.A. and Palmer,G.H. (1993) *Proc. Natl. Acad. Sci. USA*, **90**, 10932–10936.
44 Sczakiel,G., Oppenlander,M., Rittner,K. and Pawlita,M. (1992) *J. Virol.*, **66**, 5576–5581.
45 Tang,X.B., Hobom,G. and Luo,D. (1994) *J. Med. Virol.*, **42**, 385–395.
46 Cotten,M. and Birnstiel,M.L. (1989) *EMBO J.*, **8**, 3861–3866.
47 London,R.E. (1991) *Annu. Rev. Physiol.*, **53**, 241–258.
48 Sioud,M. (1994) *J. Mol. Biol.*, **242**, 619–629.
49 Knaus,T. (1995) PhD thesis, University of Heidelberg, Heidelberg, Germany.